Computer wind investigations for long bridge crossings

D. Janjic & A. Domaingo
TDV Technische Datenverarbeitung Dorian Janjic & Partner GmbH/Bentley Systems, Graz, Austria

ABSTRACT: This articles describes the necessary steps to perform computer aided layout and monitoring of wind impact on long span bridges. To this end a profound statistical description of wind as well as the characterization of wind loads is needed. In the present case the latter are computed using CFD methods by providing geometric cross section information. This information is used in the following to investigate several aero-elastic phenomena observed on existing bridges by means of computational methods. The integration of the different steps into a engineering software package is outlined and practical examples are presented.

1 INTRODUCTION

Wind impact is becoming more and more important for safety considerations of bridges, especially if crossing large rivers, estuaries or sounds with larges spans. These structures are usually very slender and therefore very susceptible to wind induced vibrations.

Many critical aero-elastic phenomena have been observed on existing bridges, and considering the risks in the design phase, as well as continuously observing related phenomena throughout life-time, have become a must for all major bridge structures. These phenomena include vortex shedding and the lock-in phenomenon, across-wind galloping and wake galloping, torsional divergence, flutter phenomena and wind buffeting etc.

Being able to deal within one software package with all related problems eases the required investigations. Once an appropriate mathematical model has been established, respective analyses for design purposes or for verifying observed phenomena and calibrating the model assumptions can be easily performed at any time. This ability was recently included in a renowned structural engineering program.

The first step is to determine the relevant aerodynamic coefficients with an integrated CFD function. Up to now, these coefficients have typically been measured in time consuming wind tunnel tests. Extensive comparisons of the CFD results with those of wind tunnel tests were used to calibrate the used discrete vortex method (DVM). The CFD analysis also allows for investigating the vortex shedding phenomenon. The program calculates the vortex shedding frequency as a function of the wind speed, and comparing it with the natural frequencies yields the critical wind speed value. Within further CFD runs with dynamic cross sections flutter derivates can be calculated. The full set of wind data can thus be prepared based on numerical simulation. The aero-elastic stability checks can be evaluated and reported.

The wind buffeting analysis is based on the above-mentioned aerodynamic coefficients and their derivatives, and on the relevant wind profile parameters (speed, direction, turbulence intensity, power spectrum, coherence data). The analysis includes aeromechanical admittance functions to define interaction between bridge and wind. Aero elastic damping and stiffness are fully included in analysis. The outlined solution procedures are implemented in commercial software package.

2 STATISTICAL DESCRIPTION OF WIND

Due to their extraordinary dimensions – with spans of 1500 m and more and pylon heights up to 200 m – the modeling of wind impact on bridges can not be solely based on one average wind velocity. As e.g. pointed out by Strømmen (2006), a complete statistical description of local wind conditions must be considered. This topic covers temporal and spatial properties in real as well as in Fourier space.

Wind loads are proportional to the squared wind velocity which varies primary with height above ground. Therefore an accurate description as possible is essential, especially for bridges with high pylons. A common wind velocity distribution is the logarithmic law which can be found also in design codes like the Eurocode. The wind velocity U obtained in this way is a mean velocity over a certain averaging interval of magnitude 10 min. Long term effects are introduced by defining season dependent additional factors.

To treat the effects of wind gusts, turbulence is characterized as well in time space in the form of turbulence intensity as in frequency space in terms of the power spectral density. The former is given by the ratio of standard deviation to average velocity and is often approximated as constant or inverse logarithmic. The power spectrum which indicates how wind energy is distributed with frequency of events is normally given in non-dimensional form, prominent examples are Kaimal type spectra (Kaimal et al. 1972) like the one presented in Figure 1.

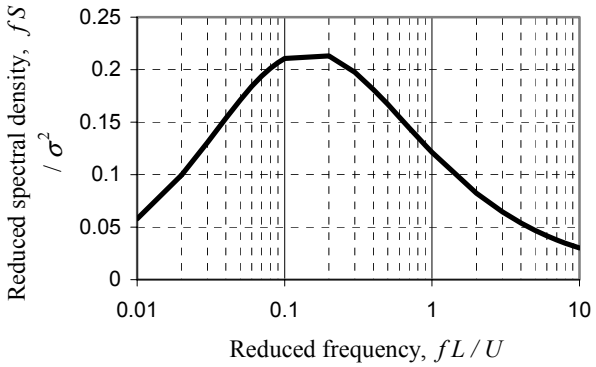

Figure 1. Typical reduced Kaimal power spectrum for turbulence component.

Another point which must be considered is the coherence of wind events along the bridge main span. For short bridges such events can be assumed to be correlated, but for long span bridges correlation must be thoroughly investigated. Normally these effects are included by providing a normalized co-spectrum, which is often of a modified exponential form as suggested by Krenk (1995).

3 AERODYNAMIC COEFFICIENTS

The time averaged forces (marked with a subscript s hereinafter) on a fixed cross section are commonly expressed by the steady state aerodynamic coefficients C_D, C_L and C_M via

$$D_s = \tfrac{1}{2}\rho U^2 \ell_D C_D \qquad L_s = \tfrac{1}{2}\rho U^2 \ell_L C_L \qquad M_s = \tfrac{1}{2}\rho U^2 A C_M \tag{1}$$

where ρ = mass density of air; ℓ_D, ℓ_L = normalization lengths; and A = normalization area. In bridge engineering it is common to relate the normalization for lift and moment to the width B of the cross section: $\ell_l = B$ and $A = B^2$. The normalization for drag is either related to cross section width B or height H. In the above equation it should be noted that the forces are given per meter of span length.

In principle the steady state coefficients are dependent both on the wind direction α and velocity U. However the cross sections used for bridges normally display less dependence on the velocity so that only the angle dependence is considered.

The time dependent lift and moment forces (with subscript t) for oscillating cross sections are expressed by the so called flutter derivatives A_i^* and H_i^* as suggested by Simiu & Scanlan (1996). The derivatives relate the resulting forces to the vertical and torsional displacements h and α, respectively, and their first derivatives with respect to time:

$$\begin{aligned} L_t &= \tfrac{1}{2}\rho U^2 \ell_L \left(KH_1^* \frac{\dot{h}}{U} + KH_2^* \frac{B\dot{\alpha}}{U} + K^2 H_3^* \alpha + K^2 H_4^* \frac{h}{B} \right) \\ M_t &= \tfrac{1}{2}\rho U^2 A \left(KA_1^* \frac{\dot{h}}{U} + KA_2^* \frac{b\dot{\alpha}}{U} + K^2 A_3^* \alpha + K^2 A_4^* \frac{h}{B} \right) \end{aligned} \tag{2}$$

where $K = b\omega / U$; and $\omega =$ circular frequency of oscillation. It should be noted that due to historical reasons the quantities are often given with inverse sign compared to the steady state coefficients, e.g. with positive sign of lift and heave in downward direction. In most practical cases the flutter derivatives are not given in dependence of the reduced frequency K, but of the reduced velocity $U_{red} = 2\pi / K$.

Finally, periodic shedding of large eddies in the wake of bluff bodies can be observed for a wide range of admissible Reynolds numbers. The frequency of vortex shedding is given in non-dimensional form by the Strouhal number St, where the normalization length is often equal to the height of the considered cross section:

$$St = \frac{fH}{U} \tag{3}$$

4 CFD CALCULATION

For any further wind related investigation an as complete as possible knowledge of the different aerodynamic coefficients is inevitable. So far, these coefficients have been determined mostly with time-consuming wind tunnel measurements. Within the last two decades the application of numerical methods has gained a high level of acceptance and importance in wind engineering. Due to increasing computational resources more sophisticated methods could be implemented. For the present considerations the so called discrete vortex method (DVM) was applied. This method was first used for analysis of bridge decks by Walther (1994) and Walther & Larsen (1997), and since then the applicability of the proposed algorithms has continuously grown.

The DVM is a suitable method to solve the Navier-Stokes equations for incompressible fluids at constant temperature, which describe the air flow around a rigid cross section. For 2D cross sections it can be simplified to yield the vorticity transport equation governing the time evolution of the vorticity field ω

$$\frac{\partial \omega}{\partial t} + (\mathbf{u} \cdot \nabla)\omega = \nu \nabla^2 \omega, \qquad \omega = \nabla \times \mathbf{u} \tag{4}$$

where $\mathbf{u}$ = velocity; and ν = kinematic viscosity of air. The boundary conditions are chosen such that the oncoming velocity far away from the cross section and the normal velocity to the cross section surface is prescribed, an approach also called the no-penetration boundary condition. Walther & Larsen (1997) point out that together with the continuity equation $\nabla \mathbf{u} = 0$ and conservation of total circulation the no penetration boundary condition is equivalent to the no slip boundary condition usually demanded in aeronautics.

The vorticity field ω is represented by a large number of vortex particles of given size σ and circulation Γ located at positions $\mathbf{x}_i$:

$$\omega(\mathbf{x}) = \sum_i \delta_\sigma (\mathbf{x} - \mathbf{x}_i)\Gamma_i \,, \tag{5}$$

where δ_σ = Dirac-Delta like core function of spread σ. The surface of the cross section is approximated by straight panels, which are associated with a linearly varying surface vorticity γ. The velocity boundary condition along the surface together with the global conservation of circulation can be used to determine this surface vorticity, which is subsequently diffused into the flow as new vortex particles.

The time integration of Equation 4 is performed by applying an operator splitting method. The first fractional step treats the convection term on the left hand side. Here the characteristics of the vortex particles are tracked in a Lagrangian manner, and a first order Euler scheme is applied to move the particles. The velocity is reconstructed from the vorticity field via the Biot-Savart relation

$$\mathbf{u}(\mathbf{x}) = U - \int \frac{\omega(\mathbf{x}_0) \times (\mathbf{x}_0 - \mathbf{x})}{|\mathbf{x}_0 - \mathbf{x}|^2} \mathrm{d}\mathbf{x}_0 \tag{6}$$

Due to the approximation of the vorticity field by a large number of N distinct vortex particles the evaluation of the integral in Equation 6 is equivalent to a $N \times N$ particle interaction which is normally related to high computational effort. Several methods have been proposed in literature to speed up calculation. Morgenthal (2002) applies a so called P^3M method. Walther (1994) uses the adaptive multipole method (AMA) following the concept of Carrier et al. (1988). This algorithm is also applied for the present implementation.

The diffusion term on the right hand side of Equation 4 is handled by a random walk method in the second fractional step. This approach was originally suggested by Chorin (1973) and is nowadays a standard tool for simulation of viscous diffusion in discrete vortex modeling (Lewis 1991).

The time dependent pressure along the cross section outline can be deduced from the vorticity flux through the surface and is used to calculate time dependent force and moment on the cross section. In a post-processing step, the time histories are analyzed to yield the time averaged non-dimensional steady state coefficients according to Equation 1 or the flutter derivatives according to Equation 2.

5 APPLICATION OF WIND LOAD

5.1 *Static wind loading*

The effect of the steady state mean wind U is applied to the structural model as uniformly distributed load along the beam elements. To this end so called "aero classes" which encapsulate the different aerodynamic coefficients related to the cross section can be assigned to the distinct beam elements. The information about mass density of air and distribution of wind velocity with height to calculate the dynamic pressure $\frac{1}{2} \rho U^2$ is attributed to different wind types. Finally the wind load on the beam elements is evaluated by combining the geometric element data with the associated aero class and wind type.

5.2 *Wind buffeting*

Next to the steady state loading described in the previous section, additional net forces my arise due to velocity fluctuations in the oncoming flow by coupling of resonant frequencies of flow and structure. To analyze this phenomenon the driving forces are decomposed into static, dynamic and aerodynamic contributions. Here dynamic loading refers to time dependent load distributions caused by the additional wind velocity components $u(t)$ along and $v(t)$, $w(t)$ normal to the wind direction. All of them have zero mean value and are characterized by a suitable power spectrum $S_{u,v,w}$. The aerodynamic contributions are additional stiffness and damping terms caused by the structural response. A full description of the buffeting forces used for the used implementation is presented in Janjic & Pircher (2004).

Since the relevant wind information is given in frequency domain the treatment of the buffeting problem is also performed in the frequency domain. First a non-linear static analysis is performed to obtain a complete set of eigenvectors and frequencies of the system in still air. The final wind buffeting analysis with prediction of resulting displacements is performed in the mo-

dal space by a convolution of the structural response spectra obtained from the eigenmode analysis and the spectrum of driving wind forces.

6 WIND DESIGN CHECKS

Depending on the cross section shape different stability and divergence phenomena have been classified. In general it can be observed that these phenomena only occur, if the aerodynamic coefficients modeling the cross section-air flow interaction match some necessary condition and if the wind velocity exceeds a critical value. Therefore, even without considering a full scale buffeting analysis, valuable design checks can be performed with simplified assumptions.

6.1 *Galloping instability*

The galloping instability is a simplified case of the buffeting analysis, where only a vertical oscillation of the cross section at low frequency is considered. Due to the motion of the cross section the effective wind velocity U_{eff} changes with time as indicated in Figure 2.

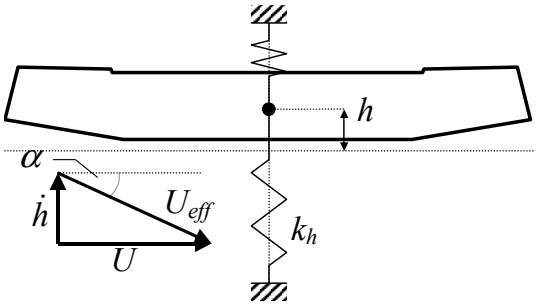

Figure 2. Simplified structural model for galloping.

The buffeting forces in this case reduce to

$$L \approx \tfrac{1}{2}\rho U_{eff}^2 \ell_L \left[C_{L0} - \frac{\dot{h}}{U_{eff}} \left(C'_{L0} + \frac{\ell_d}{\ell_l} C_{D0} \right) \right] \tag{7}$$

where the additional subscript "0" indicates horizontal wind incidence. The term in round brackets leads to an additional system damping and is known as the Glauert-Den Hartog criterion. Whenever this term becomes negative the system tends to an unstable solution. Since drag is always positive, galloping can only occur if the slope of lift is negative at $\alpha = 0$.

6.2 *Torsional divergence*

Self-driven torsional divergence may occur if the twist of the cross section induced by the aerodynamic torsional moment increases the effective wind attack angle. This in turn further increases the effective moment and so on. If the torsional stiffness of the structure is not high enough to counterbalance this increase of moment, divergence will be observed and no stable equilibrium solution is possible. By assuming a linear dependence of the moment on attack angle the critical divergence velocity reads

$$U_{c,\mathrm{div}} = \sqrt{\frac{2k_\alpha}{\rho A C'_{M0}}} \tag{8}$$

where $k_\alpha = I\,\omega_\alpha$ =torsional stiffness, I = moment of inertia; and ω_α = lowest torsional eigenfrequency.

6.3 *Classical flutter*

The term classical flutter refers to a flow driven coupled two-degree-of-freedom oscillation of the cross section. To solve the flutter problem, a coupled system of equations of motion is constituted where the forces are given by Equation 2. The critical velocity is the point of transition from damped oscillation to sustained oscillation. If the solutions are denoted in complex form, the according circular frequency at the critical velocity must be a real number and a solution can be obtained by following Simiu & Scanlan (1996). By inserting the ansatz $(h, \alpha) = (h_0, \alpha_0) \exp(\omega t)$ into the equations of motion a linear system $\mathbf{M}\cdot(h_0, \alpha_0) = 0$ is obtained. This system has non-trivial solutions only if the determinant of the coefficient matrix vanishes. Because of the used ansatz, the matrix coefficients are complex numbers and the determinant evaluates to a polynomial of fourth order in ω. By considering the real and imaginary part of this equation separately, which is possible because the frequency is real, two real polynomials of fourth and third order are established:

$$\det(\mathbf{M}) = P_4(\omega; k) \equiv P_4^r(\omega; k) + iP_3^i(\omega; k) \tag{9}$$

The coefficients of these polynomials depend on K via the involved flutter derivatives, and a common solution to both polynomials to fulfill $\det(\mathbf{M}) = 0$ is only possible for certain values of the reduced frequency K. Once such values for the reduced frequency K_{crit} and frequency ω_{crit} have been found, the critical velocity can be calculated from the definition of the reduced frequency.

6.4 *Torsional flutter*

By inspecting Equation 2 it can be observed that the terms including derivatives of h and α cause additional aerodynamic damping of the structural system. If all of the corresponding four leading flutter derivatives are negative only the coupled system may lead to sustained oscillations. For certain type of cross section, however, it has been observed that the flutter coefficient A_2^* may take positive values. In this case also one-degree-of-freedom torsional flutter becomes possible. As for galloping the critical point is at transition of positive to negative effective damping for which the following critical parameters can be derived:

$$A_{2,crit}^*(K_{crit}) = \frac{4\zeta_\alpha I}{\rho B^2 A} \quad \Rightarrow \quad U_{c,t} = \frac{B\omega_\alpha}{K_{crit}} \tag{10}$$

where ζ_α = critical damping ratio for torsion.

6.5 *Vortex shedding*

The vortex shedding phenomenon is accompanied by large oscillating lift forces of the same frequency as the shedding. Related to this problem is the so called lock-in effect, which happens if the vortex shedding frequency lies close to a natural frequency of the structure. When the corresponding eigenmode is excited, the vortex shedding frequency will be pinned to the driving frequency and massive self interaction can be observed. To estimate the effect, vortex shedding velocities $U_{c,s}$ can be derived from Equation 3 for the different natural frequencies. Design checks demand that further investigations are performed for a given natural mode if $U_{c,,x} < f_s\, U$ where f_s = additional safety factor (e.g. $f_s = 1.25$ in Eurocode).

7 PRACTICAL EXAMPLES

The Hardanger bridge will cross the fjord of same name in Norway. It is planned as a 2 lane suspension bridge with lane for bicycles and pedestrians. The bridge will have a main span of 1310 m and a total length of 1380 m. The bridge towers will elevate to 186 m above sea level. Exhaustive CFD calculations were performed to analyze the wind-bridge interactions. The obtained steady state coefficients for the main deck cross section are presented in Figure 3. Since the slope of the lift coefficient C_L is always positive, no galloping can occur.

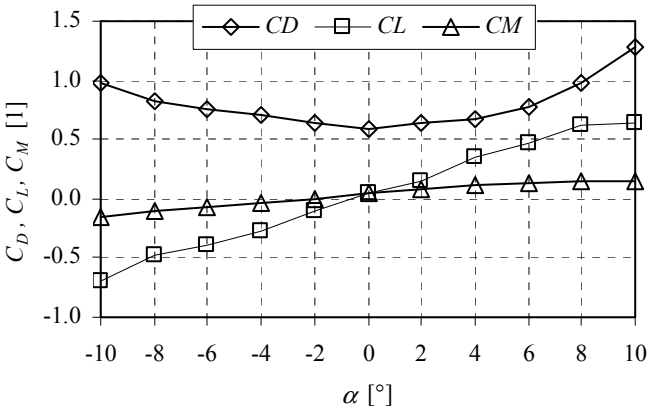

Figure 3. Steady state aerodynamic coefficients for main deck of Hardanger bridge.

Flutter derivatives have been calculated e.g. for the Great Belt East bridge in Denmark which is well documented concerning CFD calculations (cf. Walther 1994). The main span is more than 1600 m compared to a cross section width of about 32 m. The calculation results are presented in Figure 4 and Figure 5. The critical flutter velocity is evaluated to 41.8 m/s, compared to wind tunnel measurements of 37.6 m/s (Reinhold et al. 1992). Torsional flutter is not possible since the flutter coefficient A_2^* is negative for al reduced velocities.

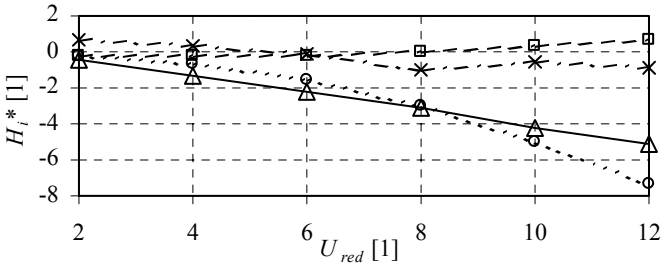

Figure 4. Flutter derivatives H_1^* (Δ), H_2^* (□), H_3^* (o) and H_4^* (x) of Great Belt bridge.

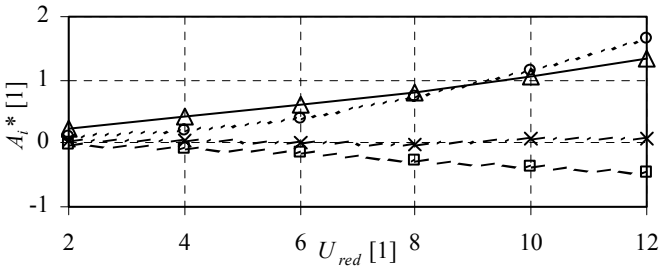

Figure 5. Flutter derivatives A_1^* (Δ), A_2^* (□), A_3^* (o) and A_4^* (x) of Great Belt bridge.

A detailed buffeting analysis has been performed for the Stonecutters bridge (Project Engineers: Ove-Arup, Hong-Kong), a cable-stayed bridge with a main span of 1018m, side spans of 298m, and a towers height of 290m. The deck to the main span is a twin girder steel deck, whilst the side spans are of concrete, which are to be built in advance of cable stay erection to counterbalance and stabilise the slender lightweight main span deck. The calculated wind buffeting responses are shown in Figure 6 to Figure 8.

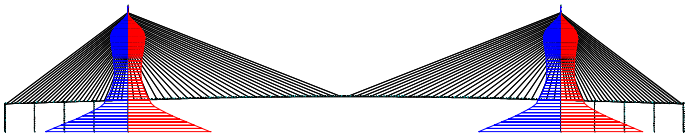

Figure 6. Tower bending moment of Stonecutter bridge due to wind buffeting.

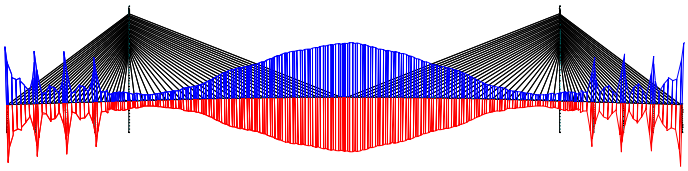

Figure 7. Deck bending moment of Stonecutter bridge due to wind buffeting.

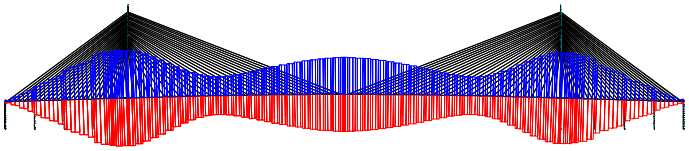

Figure 8. Deck normal force of Stonecutter bridge due to wind buffeting.

8 CONCLUSIONS

This paper describes the necessary preliminaries of sophisticates bridge design analysis. The presented considerations were implemented into a commercial structure analysis program called RM2006 and allow for a compact and time saving design process. The presented examples indicate that the proposed holistic approach is a promising way to ease further the planning of big bridge projects.

REFERENCES

Carrier, J., Greengard, L. & Rokhlin, V 1988. A Fast Adaptive Multipole Algorithm for Particle Simulations. *SIAM J. Sci. Stat. Comput.* 9: 669-686.

Chorin, A.J. 1973. Numerical Study of Slightly Viscous Flow. *J. Fluid Mech.* 57: 785-796.

Lewis, R.I. 1991. *Vortex Element Methods for Fluid Dynamic Analysis of Engineering Systems.* Cambridge: Cambridge University Press.

Janjic, D. & Pircher, H. *Consistent Numerical Model for Wind Buffeting Analysis of Long-Span Bridges*, Proc. IABSE-Symposium, Shanghai 2004.

Kaimal, J.C., Wyngaard, J.C., Izumi, Y. & Coté, O.R. 1972. Spectral characteristics of surface-layer turbulence, *Quart. J. Roy. Meteor. Soc.* 98: 563-589.

Morgenthal, G. 2002. *Aerodynamic Analysis of Structures Using High-resolution Vortex Particle Methods*. PhD Thesis. Cambridge: University of Cambridge.

Reinhold, T.A, Brinch, M. & Damsgaard, A. 1992. *Wind tunnel tests for the Great Belt Link*. Proc. First International Symposium on Aerodynamics of Large Bridges. 255 - 267.

Simiu, E. & Scanlan, R.H. 1996. *Wind Effects on Structures: Fundamentals and Application to Design*. New York: John Wiley & Sons.

Strømmen E.N. 2006. *Theory of Bridge Aerodynamics*. Berlin Heidelberg: Springer-Verlag.

Walther, J.H. 1994. *Discrete Vortex Method for Two-dimensional Flow past Bodies of Arbitrary Shape Undergioing Prescribed Rotary and Translational Motion*. PhD Thesis. Lyngby: Technical University of Denmark.

Walther, J.H. & Larsen, A. 1997. Two dimensional discrete vortex method for application to bluff body aerodynamics. *J. Wind Eng. Ind. Aerodyn* 67&68: 183-193.